

Sea surface elevation maps obtained with a nautical X-Band radar – Examples from WaMoS II stations

Katrin Hessner¹, Konstanze Reichert²

¹ OceanWaveS GmbH
Munstermannskamp 1
21335 Lüneburg , Germany
Email: hessner@oceanwaves.de

² OceanWaveS Pacific Ltd.
23 Corrondella Gr
Belmont – Lower Hutt
New Zealand

The Wave Monitoring System WaMoS II was developed for real time measurements of directional ocean wave spectra. It has been used in recent years to monitor the sea state from fixed moored platforms, coastal areas and moving vessels.

WaMoS II uses *sea clutter* information which represents the backscatter of microwaves from the sea surface in nautical radar images. By analyzing the sea clutter the directional wave spectra can be obtained. From such spectra all spectral sea state parameters such as significant wave height, peak period, and peak direction both for wind sea and swell can be derived.

In addition to the spectral wave parameters, WaMoS II has been extended to derive series of sea surface elevation maps. These surface maps allow to investigate the properties of individual waves in time and space. A directional wave finding algorithm allows to determine amplitude and phase of each partial wave of the wave spectrum. This algorithm was applied to a number of different data sets. Several parameters can be derived from the sea surface elevation maps that give a better understanding of the individual wave structure. For example studies on the observed maximal wave heights can be carried out for different wave scenarios. Interesting aspects are the temporal evolution of the ratio between occurring maximal and significant wave heights during a developing storm.

Initially the development of the algorithms was started with special emphasis on 'extreme waves'. The need to better understand the nature and the probability of occurrence of such events led to a range of ongoing R&D studies. Mostly those applications are of interest for ship applications with the aim to predict the ship movements over varying temporal scales. Most of the development work is initially tested for fixed stations. In Oct./Nov. 2006 an extreme wave event caused some damage on a platform in the Southern North Sea. WaMoS II radar raw data from this platform will be presented, giving an impression of those area covering measurements that allow for looking at the evolution of waves in space and time.

1 INTRODUCTION

Wave information is usually derived from time series of the sea surface elevation measured at a certain location in the open sea. These measurements are carried out by in-situ sensors such as buoys, lasers, and pressure sensors with high temporal resolution (e.g., sampling frequencies of about 2Hz). However, deployments of such sensors are limited by the local water depth, as well as the mooring facilities. For instance buoys can be easily damaged by ships or during severe storm conditions. Furthermore, the use of point measurements assumes

that the obtained wave information is representative for a particular area, which is often not the case, especially in coastal waters, where coastal effects like wave refraction, diffraction, shoaling etc. take place. Under these conditions, the sea state can vary significantly in space. Complementing point measurements, the imaging of the sea surface based on remote sensing techniques provides information about the spatial variability of the sea. One of these techniques is based on the use of ordinary nautical X-band radars to analyze ocean wave fields.

Under various conditions, signatures of the sea surface are visible in the near range (less than 3 nautical miles) of nautical X-band radar images. These signatures are known as sea clutter, which is undesirable for navigation purposes. Therefore, the sea clutter is generally suppressed by filtering algorithms. Sea clutter is caused by the backscatter of the transmitted electromagnetic waves from the short sea surface ripples in the range of half the electromagnetic wavelength (i.e. ~ 1.5 cm). The longer waves like swell and wind sea become visible as they modulate the backscatter signal mainly via hydrodynamic modulation of the ripples by the interaction with the longer waves, tilt modulation due to the changes of the effective incidence angle along the long wave slope, and the partial shadowing of the sea surface by higher waves (Keller and Wright, 1975, Alpers et al., 1981; Plant, 1990; Wenzel, 1990; Lee et al., 1995).

Since standard X-band nautical radar systems allow the sea surface to be scanned with high temporal and spatial resolution, they are able to monitor the sea surface in both time and space. The combination of the temporal and spatial wave information allows the determination of unambiguous directional wave spectra. In addition to point measurements techniques nautical radar imagery also permits the observation of spatial variations in the wave field. Furthermore, the use of nautical radar as a remote sensor enables the measurement of wave field features from moving vessels.

In the past different systems using nautical radars for measuring sea states have been developed. This paper focuses on one of these devices, the German system WaMoS II (**Wave Monitoring System**), which is described in the following section.

The paper is designed as following: First a brief introduction to the standard WaMoS II is given. Then the inversion scheme and the possibilities of the sea surface elevation maps are given. Finally a hazard storm case with extreme waves is presented. The data presented in the paper is obtained by the FINO 1 platform located in the German Bight.

2 THE WAMOS II SYSTEM

WaMoS II is a high-speed video digitizing and storage device that can be interfaced to any conventional navigational X-band radar and a software package running on a standard PC. The software controls the radar and data storage. In addition, the WaMoS II software carries out the wave analysis and displays the results (see Figure 1).

The system was developed at the German GKSS Research Centre and the equipment was first tested in 1991. The technology was transferred to OceanWaves GmbH in order to market and commercialize the system. Since then WaMoS II has been improved and expanded to cover ship and shallow water applications. Since 2001 the system has been type approved by the Germanischer Lloyd and Det Norske Veritas. During several applications WaMoS II proved to be a powerful tool to monitor ocean waves from fixed platforms as well as from moving vessels, especially under extreme weather conditions (Young et al., 1985; Ziemer and Günther, 1994; Nieto-Borge et al., 1999, Hessner et al., 2001).

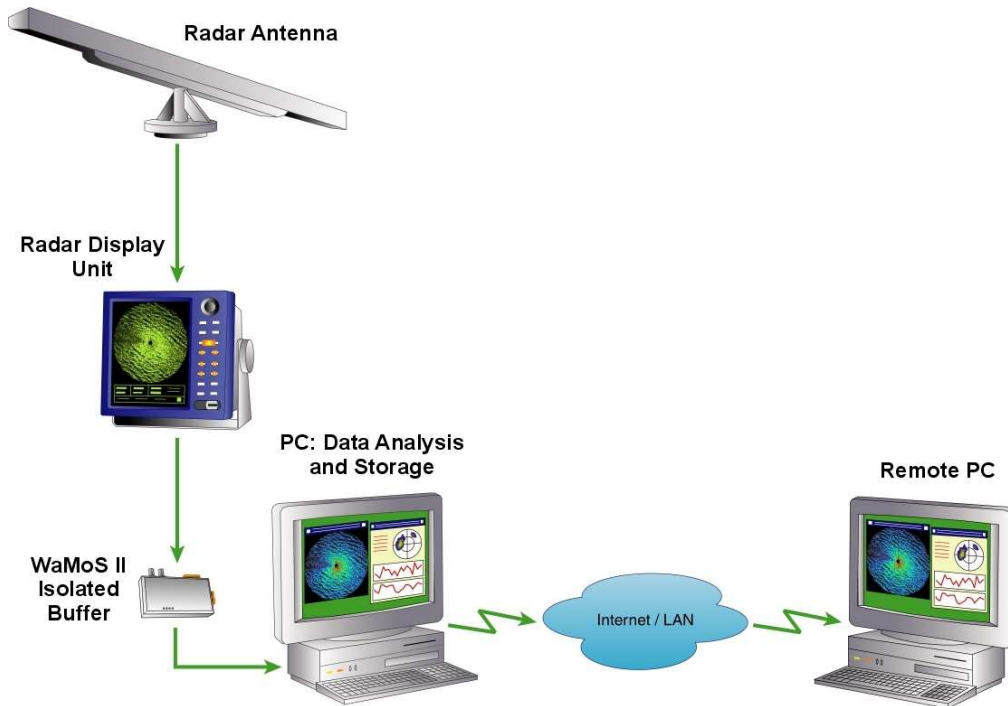


Figure 1: Schematic of the different parts of WaMoS II and the data flow from the radar antenna to the user display.

A typical WaMoS II wave measurement consists of the acquisition of a radar image sequence and the subsequent wave analysis. The sea clutter image sequence is transformed into the spectral domain by means of a three dimensional *Fast Fourier Transform* (FFT). First the surface current is estimated from the image spectrum by means of a least-squares-method using the dispersion relation for linear water waves as reference. Then the dispersion relation including the current component (Doppler term) is used to separate wave related spectral information from noise. Finally, by applying a modulation transfer function the wave spectrum is determined. From this wave spectrum all kinds of commonly used types of wave spectra can be derived (wave number spectrum, frequency direction spectra, frequency spectra, etc) and various standard spectral wave parameters can be inferred.

The standard WaMoS II software delivers unambiguous directional wave spectra and time series of the integrated standard wave parameters like significant wave height (H_s), peak wave period (T_p), peak wave direction (θ_p) and peak wave length (λ_p) in real time. These data can be made available to the user on the WaMoS II PC and can also be transferred to other stations via Internet, LAN, NMEA etc.

3 OFFSHORE SEA-STATE MEASUREMENTS IN THE NORTH SEA

Within the framework of the German FINO program the first platform FINO 1 has been in operation since September 2003 (see Figure 2). The platform is located in the Southern North Sea. The aim of the project is to record precise measurements of the meteorological conditions in the lower atmospheric boundary layer. A WaMoS II was installed to investigate the load and stability of the structure due to surface waves and currents.

The atmospheric and hydrographic measurements provide important input for the design of offshore wind turbines. Further this data is used to improve atmospheric and oceanographic models thereby form the basis for the safe and economical operation of wind turbines on the open sea (Herklotz, 2007).



Figure 2: The FINO 1 platform. The nautical radar antenna used for the WaMoS II measurements is installed below the helicopter deck .

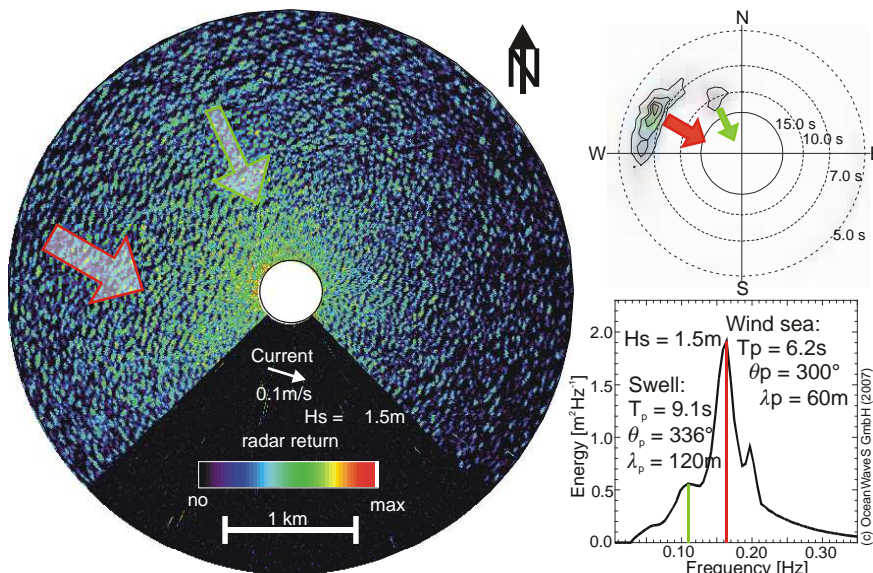


Figure 3: Radar images measured on board FINO 1 on Feb. 7th, 2006 00:09 UTC. On the right the corresponding wave spectra and spectral wave parameter as obtained by WaMoS II are given.

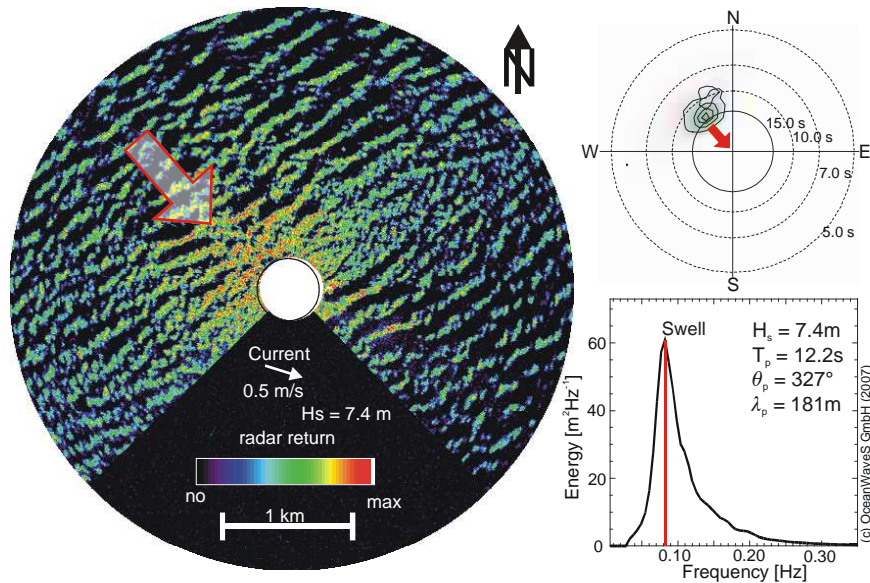


Figure 4: Same as Figure 3, but for Feb. 8, 2006, 17:00 UTC.

Figure 3 and Figure 4 show examples of radar images with sea clutter and the corresponding wave spectra determined by WaMoS II. The first example represents a bimodal sea state with a dominant wind sea (red) and secondary swell (green), while the second example shows a well developed swell.

The time series of H_s , T_p and θ_p represented in Figure 5 were obtained by WaMoS II (red) and a Waverider buoy (blue) deployed next to the FINO 1 platform. A good agreement between the WaMoS II and the buoy measurements can be seen. Slight deviations can be expected, as WaMoS II delivers spatial mean wave parameters while the buoy delivers wave parameters measured at one point.

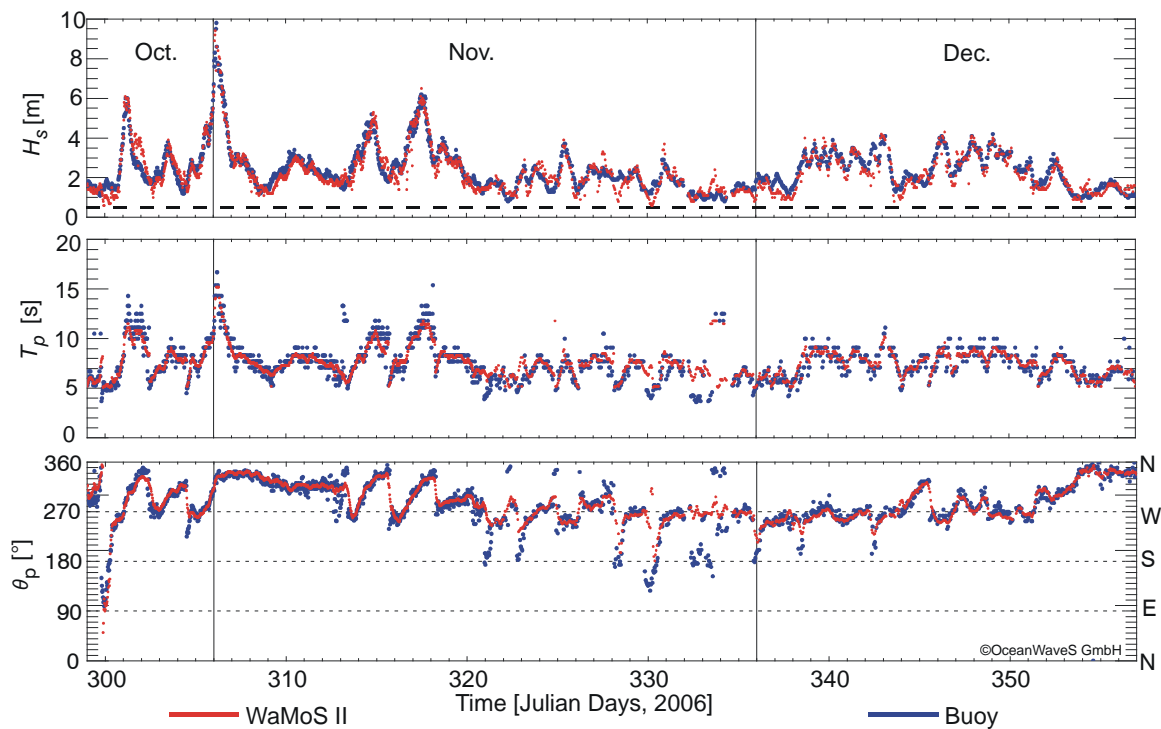


Figure 5: Comparison of the significant wave height (H_s ; top), peak wave period (T_p ; middle) and peak wave direction (θ_p ; bottom) time series obtained by WaMoS II (red) and a Waverider buoy (blue) at FINO 1.

4 SEA SURFACE ELEVATION MAPS

4.1 Inversion scheme

To retrieve sea surface elevation maps, sequences of nautical radar images were inverted by applying the method proposed by Nieto et al. (2004). This approach considers shadowing to be the main imaging mechanism of ocean gravity waves (wind sea and swell) in nautical radar images and is based on linear wave theory. It is assumed that the sea surface elevation consists of a linear superposition of several individual sinusoidal waves. By means of a FFT, a band pass filter based on the gravity wave dispersion relation, and the application of a transfer function, amplitude (A_i) and phase (ϕ_i) of a number of individual sinusoidal waves (N) are determined. The surface elevation $\eta(\mathbf{x}, t)$ at a given point an time is than given by

$$\eta(\mathbf{x}, t) = \sum_{\mathbf{k}, \omega} A_i \cos(\mathbf{k}_i \mathbf{x} - \omega_i t + \phi_i), \quad (1)$$

where \mathbf{x} is the position vector, t the time, \mathbf{k} the wave vector, ω the angular wave frequency.

To retrieve sea surface elevation maps there are two possibilities: a) inverse FFT or b) the summation of all individual wave components. The first method has the advantage that it is very fast but the results are restricted to the spatial and temporal resolution of the original radar data. The second method allows the free choice of temporal and spatial resolution and further to distinguish between encounter or real wave field which is of importance in the case of ship applications. Nevertheless this method is very time consuming.

4.2 Application

For practical purposes the inversion of nautical radar images is applied to sub areas of the radar images. These areas are aligned with respect to the peak wave direction. Figure 6 shows an example of a radar image (left), and the corresponding sea surface elevation (middle), and on the top right panel gives the orientation of the sub area with respect to the full radar image.

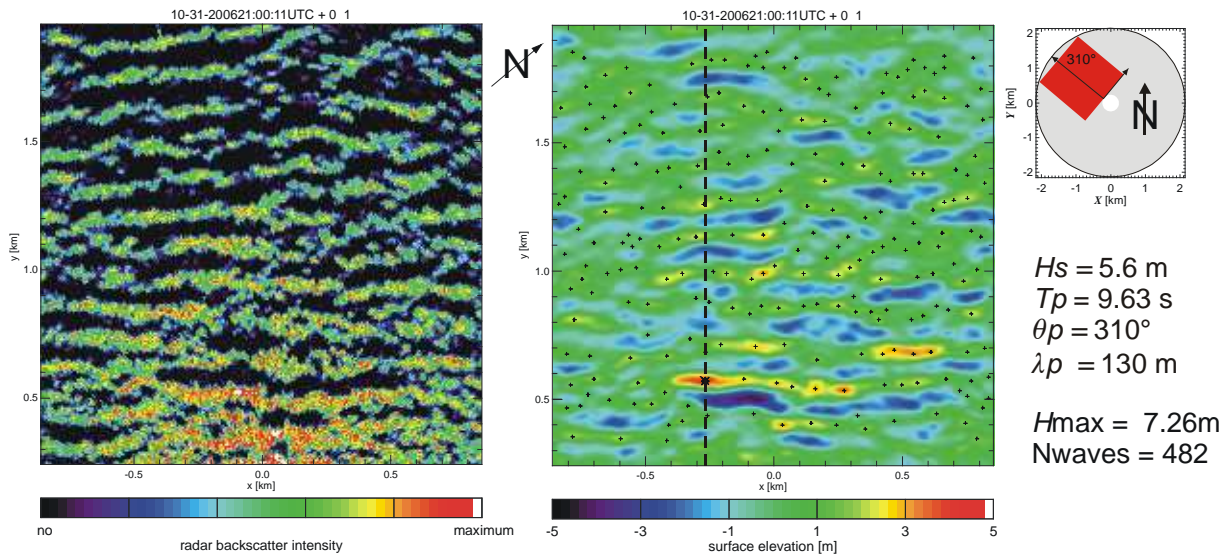


Figure 6: Area of radar backscatter intensity (left) and corresponding sea surface elevation (middle). The color coding refers to radar backscatter and surface elevation, respectively. The sketch (right) indicates the area with respect to the radar view field. The data was collected on Oct. 31, 2006, 21:00 UTC at FINO 1. The individual waves are marked with crosses, the highest wave is marked with a diamond, the dashed line indicates the location of the transect for which the wave evolution is presented.

As the sub area was chosen with respect to the peak wave direction (here 310° relative to North) the visible wave pattern are aligned parallel to the x-axis. The front side of the waves are characterized by high radar backscatter intensity while the backside and troughs show low or no radar backscatter. At that time WaMoS II measured 5.6 m significant wave height (H_s) and a peak wave period (T_p) of 9.63 s. The peak wave direction (θ_p) was 310° and the peak wave length (λ_p) 130 m. In the surface elevation maps the location of the crests of 482 individual waves are marked. These waves were found with the directional individual wave finding algorithm (DWFA; Reichert, 2006). The highest wave and crest are mark with a diamond and star, respectively. For this example the DWFA found a maximum wave height with $H_{max} = 7.26$ m.

At the location of the maximum wave a transect (dashed line) was made in wave propagation direction (see Figure 7 left panel).

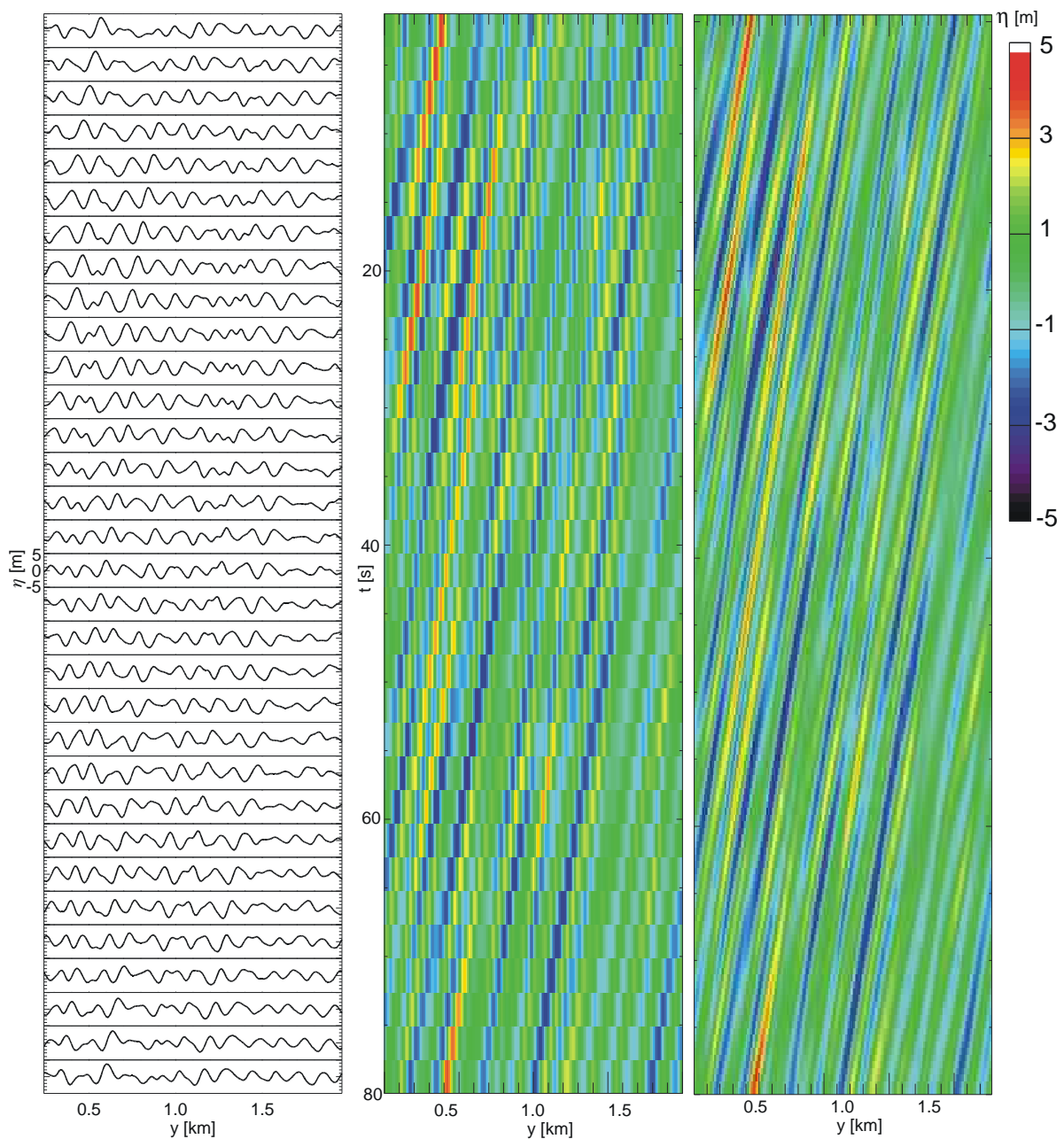


Figure 7: Left: Surface elevation as function of space along the transect (see Figure 6) and of time during one set of 32 radar rotations (y-axis). The images show the surface elevation color coded, where the middle panel is also in the same temporal resolution as the radar while the right one was determined with $dt = 0.5s$.

Figure 7 shows the wave evolution along the transect, where left the individual surface elevation as function of space and time for a set of 32 images is presented. Middle and right shows the surface elevation color coded. The middle image displays the wave evolution with the same temporal resolution as the radar data was collected ($dt = \text{radar repetition rate} = 2.5 \text{ s}$). The right image shows in same period of time but with a higher temporal resolution of $dt = 0.5 \text{ s}$.

4.3 Individual wave analysis

In Figure 8 the results of the DWFA for the surface elevation map shown in Figure 6 is given. The statistical distribution of the wave height within the area is in good agreement with the theoretical presumptions. This proves the general reliability of the DWFA results.

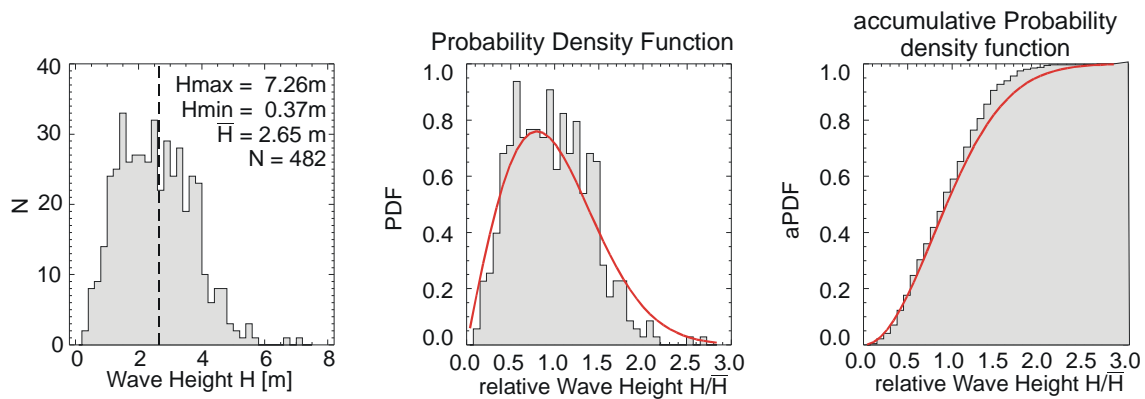


Figure 8: Wave height distribution for the sea surface elevation map shown in Figure 6. Left the Histogram for the waves.

5 EXTREME STORM EVENT NOV. 2006

An extreme event occurred in the night of Oct. 31/ Nov. 1, 2006 in the German Bight. The low pressure system BRITTA with strong and long lasting north westerly winds created a sea state in the German Bight with significant wave heights (H_s) in the range of 8-10 m. At Nov. 1, 3:30 UTC a maximum H_s up to 10.54 m were recorded by a Wave Rider buoy deployed next to the FINO 1 platform. The situation were further stressed by an extreme water level rise of 2.2 m above normal high water. Single waves hit the platform lower working deck at 11 m above the actual water level, causing damages, where several floor gratings were tore off their mountings, and parts of the railings were heavily deformed (see Figure 9) .



Figure 9: Pictures of the FINO 1 platform showing the damages due to wave impact. (©BSH)

Even structures above the lower working platform, up to about 15 m above water level, were damaged within the storm. Hence during the storm extreme waves with a crest height between 11 and 16 m had been occurred (Herklotz, 2007).

Figure 10 shows the significant wave height within the storm from Oct. 31, 13:00 – Nov.1, 16:25 UTC. The measurements of WaMoS II and buoy show general good agreement. Small deviations can be explained by the difference in the measurement technique.

During the time of maximum wave heights, the wave measuring system installed in the buoy was blocked at maximum expansion for several minutes, causing failure of the single-wave recording mechanism. Therefore, the computed significant wave height cannot be considered realistic during the whole storm period. Within the storm 4 cases of such irregularities were observed. These periods are marked grey in Figure 10.

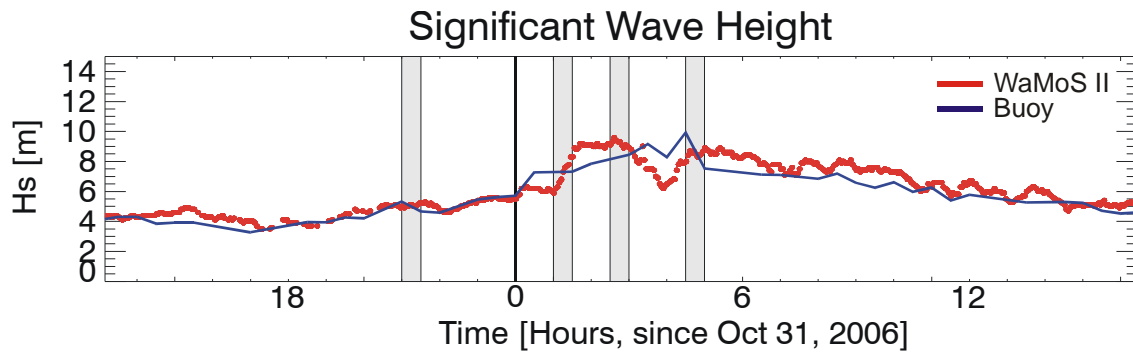


Figure 10: Time series of significant wave height as obtained by the Buoy (blue) and WaMoS II (red) for the time of the peak of storm Britta.

For the last of the four cases (Nov 1, 4:00 UTC) the time series of the vertical and horizontal elevation measured by the buoy is shown in

Figure 11.

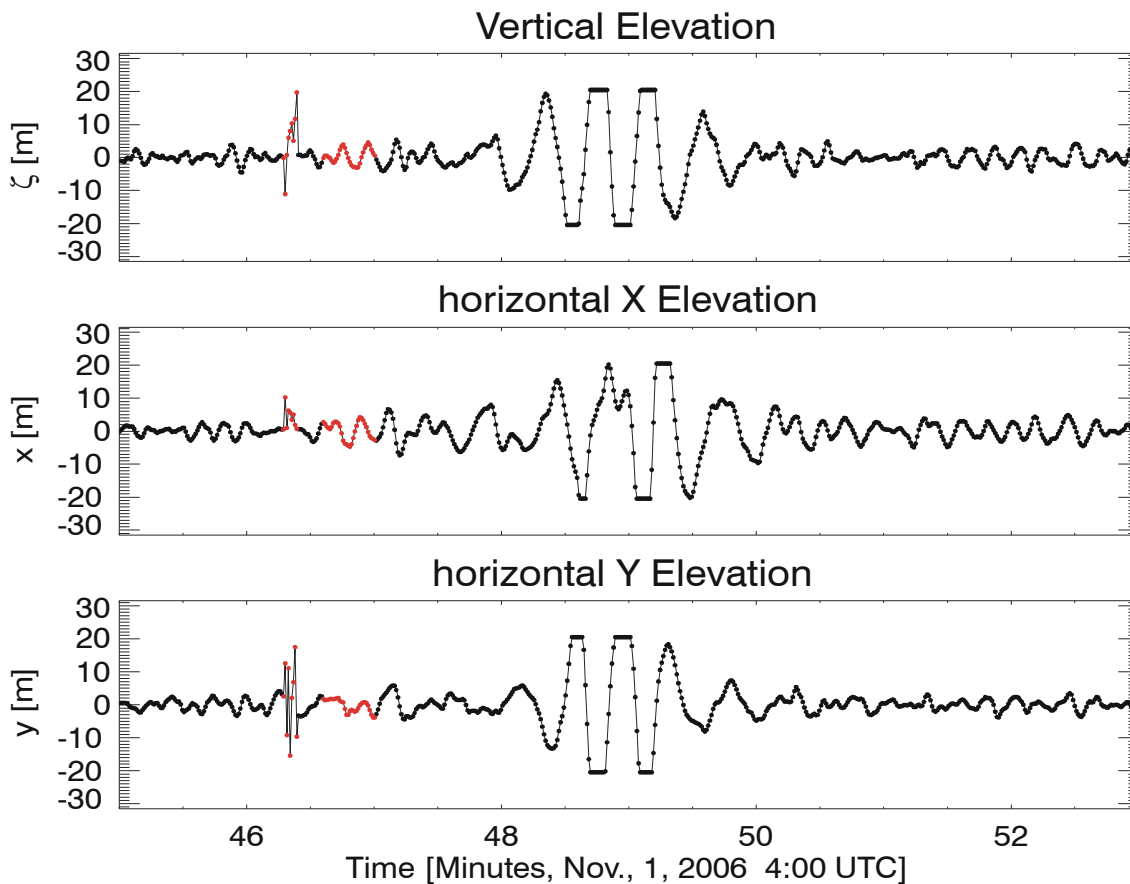


Figure 11: Time series of vertical and horizontal displacement of the buoy. The red dots indicate system failure.

The time series show that the buoy experienced an unrealistic displacement which reaches the system maximum value of 20 m. Not all of these events are marked as unrealistic by the system (red dots). Anyway these events indicate that during the storm extreme waves appear.

Figure 12 shows the maximum wave height as obtained by the DWFA from WaMoS II sea surface elevation maps (red) and by the buoy (blue) for the period from Oct. 31, 13:00 – Nov.1, 16:25 UTC. The results of the DWFA show a scattering of about 4 m. This scattering is that high because the variation of wave heights within space for are relative short time (80 s) is higher relative to point measurements over a relative long period of 30 min like the buoy measurements. Nevertheless both sensors show a good agreement with respect to range and trend. This shows an increasing maximum wave height at the beginning of the storm and decreasing maximum wave height after the peak of the storm on Nov. 1, 3:30 UTC. For the shown time series a maximum wave height of 20.57 m was measured on Nov. 1, 2:15 UTC. The corresponding radar image as well as the sea surface elevation show some cross sea feature, which gives a good explanations for a localized extreme wave event.

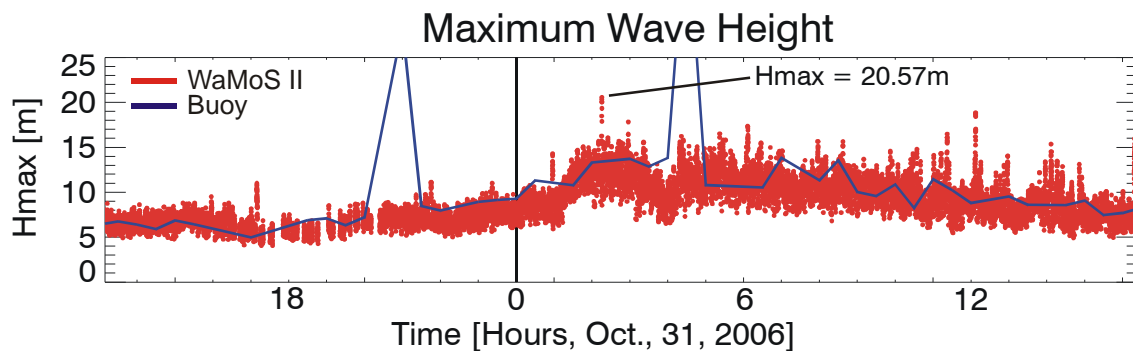


Figure 12: Time series of maximum wave height recorded during the BRITTA storm event Oct. 31/Nov. 1, 2006 by a Wave Rider buoy (blue) and WaMoS II (red) at FINO 1.

Relevant for the damages of the FINO 1 are the crest heights of the individual waves. Therefore the maximum crest heights as determined by the DWFA from the WaMoS II sea surface maps are shown in Figure 13. Like for the wave height the crest heights show a significant scatter, which can be explained by the higher spatial variability of this parameter. In particular cases, extreme high wave crests were found aside from the general trend. Within the shown time, a maximum crest height of 11.72 m was measured also on Nov. 1, 2:15 UTC. This indicates that within the storm individual waves with a crest heights above 11 m occurred in this area.

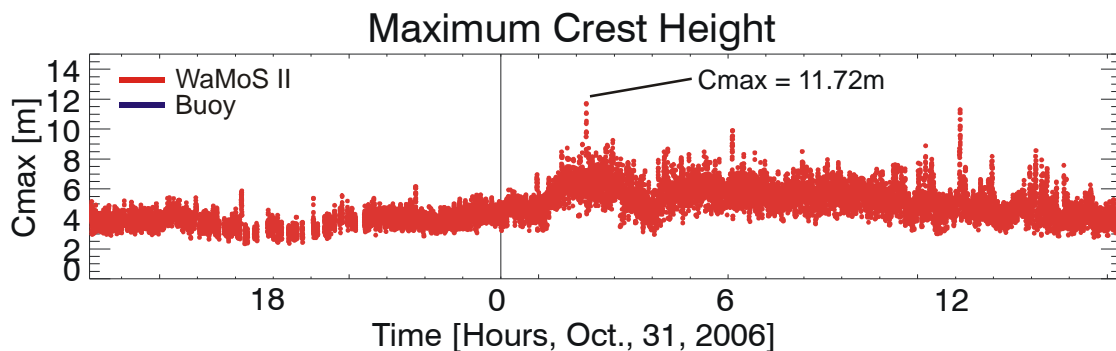


Figure 13: Time series of maximum crest height determined during the BRITTA storm event Oct. 31/Nov. 1, 2006 by WaMoS II (red) at FINO 1.

These extreme waves are very temporary and spatial localized features. Figure 14 gives a view of this extreme wave for different view angles. It is visible that the top of the wave crest is a very pointy feature in space. It was created by a sum of two wave components hitting each other. The first and main wave component is propagating in peak wave direction (red arrow). In the right panel the orientation of a secondary wave component is high lighted by a dashed line. Its propagation direction (grey arrow) is approximately 20° apart from the peak direction. The maximum wave is located where the crests of the two wave systems hit each other.

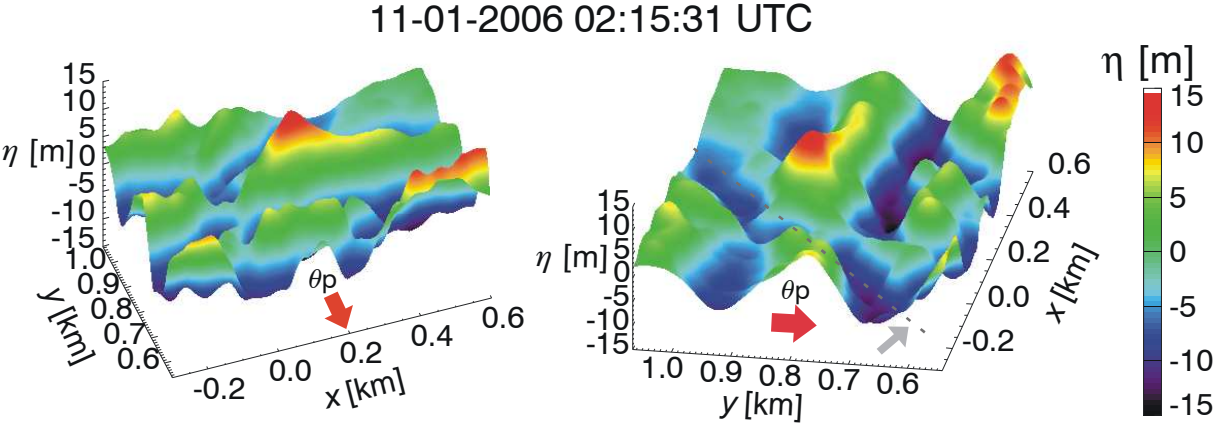


Figure 14: 3d picture of the highest wave as obtained from WaMoS II sea surface elevation maps for different view angle. The color coding represents the surface elevation. The peak wave direction (θ_p) is indicated by the red arrow. A secondary wave component is high lighted by the grey dashed line. Its direction is indicated by the grey arrow.

The inversion scheme allows to study the temporal evolution at a particular point. Figure 15 shows the sea surface elevation as function of time at the location where the maximum crest occurred.

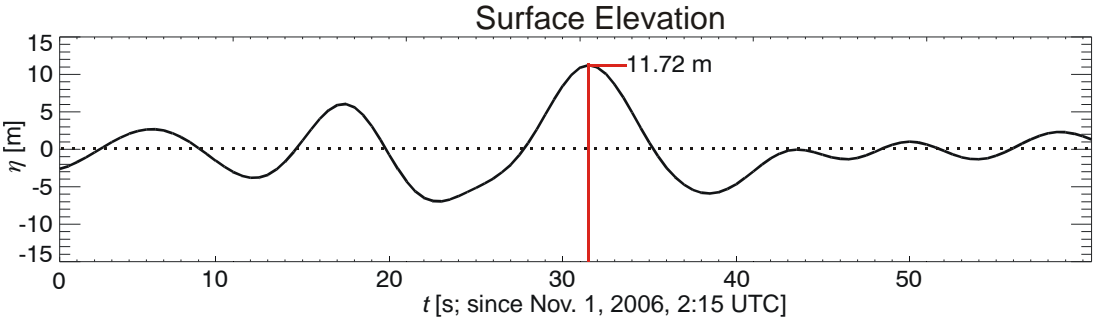


Figure 15: Time series of the sea surface elevation as obtained by WaMoS II inversion at the point where the maximum wave crest occurred. The red line marks the location of the maximum wave.

As the radar images do not cover the near field of the platform ($R < 240\text{m}$) it was not possible to determine extreme waves directly at the platform. Anyway the analysis give an idea of the general possibilities to use surface elevation maps.

6 SUMMARY AND CONCLUSION

In the paper a brief introduction to the standard WaMoS II and its deployment onboard the FINO 1 platform in the North Sea is given. Furthermore the inversion scheme, which allows to determine maps as well as time series of the sea surface elevation is stated. Results of the directional individual wave finding algorithm (DWFA), which allows to identify individual waves in sea surface maps, are presented.

A case study for an extreme storm event in the night Oct. 31/ Nov. 1, 2006 in the German Bight is presented. In this night a maximum significant wave height of 10.54 m was recorded by a buoy. The FINO 1 platform was damaged in a height of 11-16 m above the current water level. Time series of maximum wave and crest heights calculated from WaMoS II sea surface elevation maps and DWFA were presented. The maximum wave height shows a higher variability but is in general good agreement with the corresponding buoy parameter. The information about the maximum crest height yields extreme waves up to 11.72 m on Nov. 1, 2:15 UTC. The corresponding sea surface elevation map shows that this extreme wave was a spatially very localized phenomenon. The information about the wave environment indicates that this extreme wave was created by a superposition of two wave systems.

As the radar images do not cover the near field of the platform it was not possible in this study to determine surface elevation directly at the platform. The application of wave propagation algorithms may allow this in the future.

7 ACKNOWLEDGEMENTS

The work has been done within the German funded Project LaSse (Weiterentwicklung von Auswertemethoden zur Einzellwellenerkennung aus nautischen X-Band Radardaten FKZ 03SX218E). The data presented was kindly provided by the Federal Maritime and Hydrographic Agency (BSH), Germany.

8 REFERENCES

- Alpers, W., D.B. Ross, and C.L. Rufenach, 1981: On the Detectability of Ocean Surface Waves by Real and Synthetic Aperture Radar. *Journal of Geophysical Research*, 86, C7, pp. 6481-6498.
- Herklotz K., 2007: Oceanographic Results of Two Years Operation of the First Offshore Wind Research Platform in the German Bight - FINO1. *DEWI Magazin* 30.
- Hessner K., K. Reichert, J. Dittmer, J.C. Nieto Borge, and H. Günther, 2001: Evaluation of WaMoS II Wave data, *Proceedings of the Waves 2001 Conference*, Sep. 1-6, San Francisco.
- Keller W.C., Wright J.W. (1975) Microwave scattering and the straining of wind-generated waves, *Radio Science*, 10: 139-147
- Lee, P.H.Y., J.D. Barter, K.L. Beach, C.L. Hindman, B.M. Lade, H. Rungaldier, J.C. Shelton, A.B. Williams, R. Yee, and H.C. Yuen, 1995: X-Band Microwave Backscattering from Ocean Waves. *Journal of Geophysical Research*, 100, C2, pp. 2591-2611.
- Nieto Borge, J.C., K. Hessner, and K. Reichert, 1999: Estimation of the Significant Wave Height with X-Band Nautical Radars. *Proc. OMAE Conference*.
- Nieto, J.C. G.R. Rodríguez, K.Hessner, P. I. González, 2004: Inversion of Marine Radar Images for Surface Wave Analysis. *Journal of Atmospheric and Oceanic Technology*, 21, 1291-1300.
- Plant, W.J., 1990. Bragg Scattering of Electromagnetic Waves from the Air/Sea Interface, in *Surface Waves and Fluxes: Current Theory and Remote Sensing*, edited by G.L. Geernaert and W.J. Plant, Kluwer Academic Publishers, 2, p. 41-108.
- Reichert K., Hessner K., J. Dannenberg, and I. Traenkmann, 2006: X-Band Radar as a Tool to Determine Spectral And Single Wave Properties: *Proceedings of OMAE2006 25th International Conference on Offshore Mechanics and Arctic Engineering June 4-9, 2006, Hamburg, Germany*
- Wenzel, L.B., 1990: Electromagnetic scattering from the sea at low grazing angles. *Surface Waves and Fluxes*, G.L. Geernaert and W.J. Plant, Eds, Kluwer Academic, 41-108.
- Young, I.R. W. Rosenthal, and F. Ziemer, 1985: Three-dimensional analysis of marine radar images for the determination of ocean wave directionality and surface currents. *J. Geophys. Res.* 90, 1049-1059.
- Ziemer F., Günther H. (1994) A system to monitor ocean wave fields. *Proc. 2nd Int. Conf. Air-Sea Interaction Meteorol. Oceanogr. Coastal Zone*, Lisboa, September 22-27, 1994.